ACS SyntheticBiology

Research Article

pubs.acs.org/synthbio

Preventing T7 RNA Polymerase Read-through Transcription—A Synthetic Termination Signal Capable of Improving Bioprocess Stability

Juergen Mairhofer,[†,‡,§] Alexander Wittwer,[†,‡,§] Monika Cserjan-Puschmann,[†,‡] and Gerald Striedner*[,†,‡]

[†]Department of Biotechnology, University of Natural Resources and Life Sciences, Muthgasse 18, A-1190 Vienna, Austria

[‡]Austrian Centre of Industrial Biotechnology GmbH (ACIB), Petersgasse 14, A-8010 Graz, Austria

Supporting Information

ABSTRACT: The phage-derived T7 RNA polymerase is the most prominent orthogonal transcriptions system used in the field of synthetic biology. However, gene expression driven by T7 RNA polymerase is prone to read-through transcription due to contextuality of the T7 terminator. The native T7 terminator has a termination efficiency of approximately 80% and therefore provides insufficient insulation of the expression unit. By using a combination of a synthetic T7 termination signal with two well-known transcriptional terminators (rrnBT1 and T7), we have been able to increase the termination efficiency to 99%. To characterize putative effects of an enhanced termination signal on product yield and process stability, industrial-relevant fed batch cultivations have been performed. Fermentation of a *E. coli* HMS174(DE3) strain carrying a pET30a derivative containing the improved termination signal showed a significant decrease of plasmid copy number (PCN) and an increase in total protein yield under standard conditions.

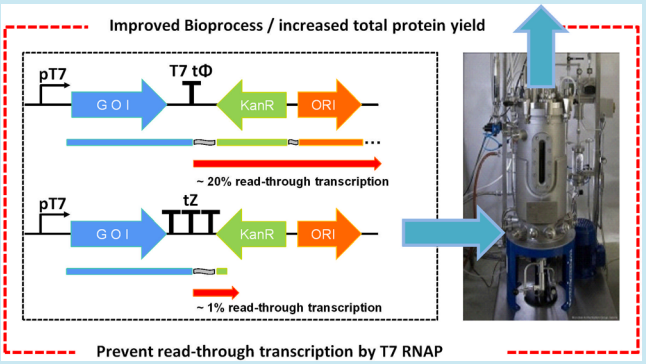

KEYWORDS: *recombinant protein expression, plasmid vector design, T7 RNA polymerase, contextuality, T7 terminator, read-through transcription, insulator*

The phage derived T7 RNA polymerase (T7RNAP) is an important molecular tool of continuing interest since the early days of genetic engineering. It has been extensively used for recombinant protein expression after it was first cloned in 1984,[1] and due to its orthogonal nature, it has become popular for synthetic biology applications. The recent years have seen research to generate orthogonal transcription−translation networks,[2] split T7RNAPs[3] or T7RNAPs with different DNA binding specificities.[4]

For most applications, the gene of interest (GOI) is cloned in a plasmid under control of the strong T7 promoter. Orthogonal transcription of the GOI is driven by the T7RNAP that is integrated into the host genome using the DE3 lambda prophage and under the control of the IPTG-inducible *lacUV5* promoter. For termination of transcription the class I intrinsic, major late T7 terminator, TΦ, is utilized historically.[5] Class I transcription termination signals are characterized by a stable hairpin structure and the immediately following oligo(U) sequence.[6] TΦ has a termination efficiency (TE) of approximately 74%,[7] and read-through transcription is actually required as there is no promoter between TΦ and the essential genes 11 and 12 in the nucleotide sequence of bacteriophage T7.[8] The biotechnological consequence of using TΦ for recombinant protein expression or in synthetic devices has been mostly disregarded so far, although some reports on the detrimental effects on read-through transcription by T7RNAP do exist in the literature.[5,9,10] Although transcription terminators are known to play a key role in regulating genetic systems the systematic study of different termination signals has just begun.[11,12] According to these studies the TE is significantly influenced by the proximal sequence context upstream and downstream of the stable stem-loop structure.

In a recent publication, we have provided evidence for a massive transcriptional read-trough by T7RNAP when the GOI was integrated into a defined locus on the genome.[13] Eight genes on the sense strand, downstream of the integration site of the GOI, were significantly up-regulated, corresponding to a region as large as 32 kbp. This is an interesting finding due to the fact that this read-through can substantially disturb the functionality of the host cell when the integration site is, for example, in proximity to regulators or genes with critical expression levels. When a plasmid-based expression system is used read-through by T7RNAP leads to up-regulation of backbone sequences.[13] This read-through can affect expression of downstream elements such as antibiotic resistance genes,

Received: January 14, 2014
Published: May 14, 2014

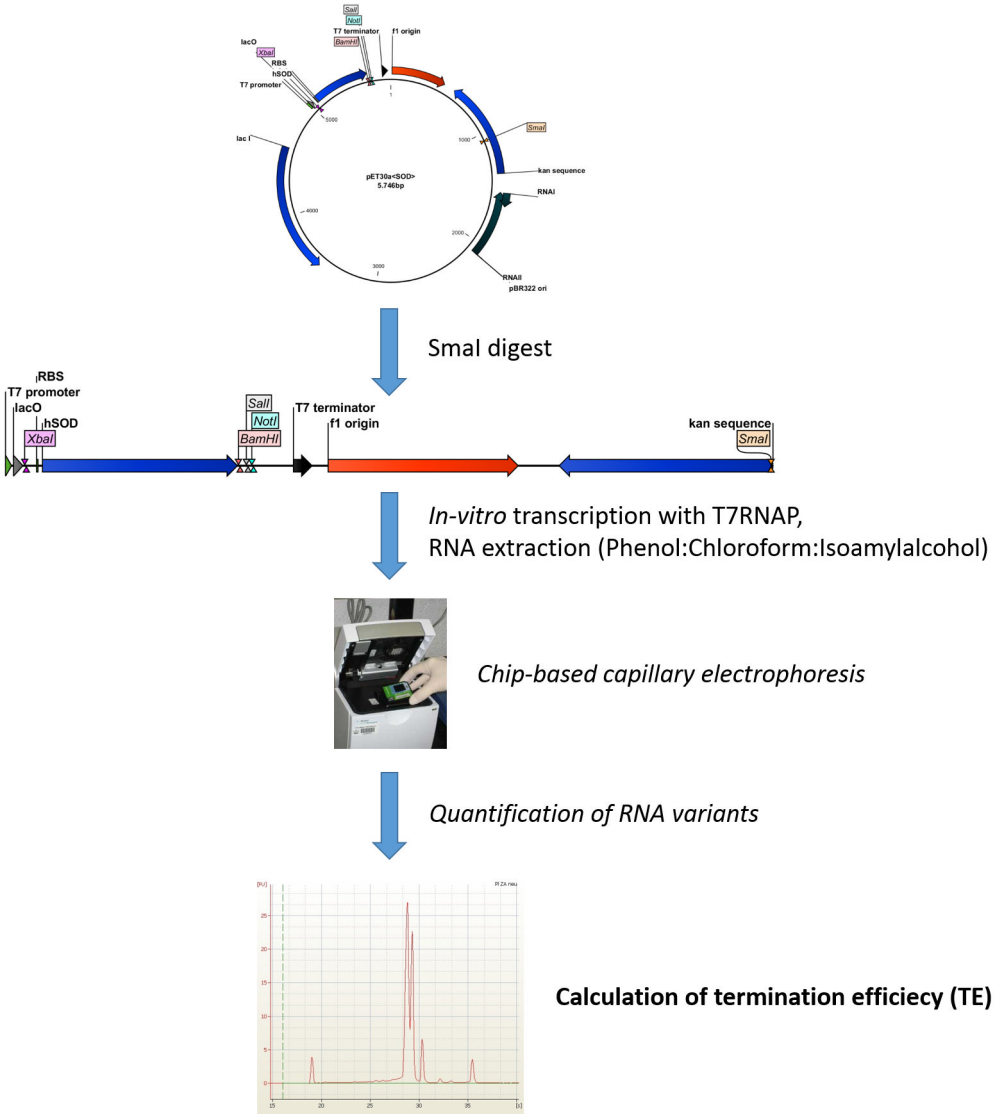

Figure 1. Overview on the procedure for the determination of the termination efficiency (TE). Plasmids have been linearized using *Sma*I, linearized dsDNA has been used as a template for *in vitro* transcription using recombinant T7RNAP. RNA has been extracted using phenol/chloroform/isoamylalcohol and was further purified using 70% and 90% ethanol solutions. Purified RNA was analyzed using chip-based capillar electrophoresis. RNA variants due to read-through transcription have been quantified and TE has been calculated accordingly.

plasmid copy number (PCN) control elements, or repressor proteins used to lower basal expression levels.

We believe that physical composition of an expression plasmid does heavily influence plasmid stability and overall bioprocess performance. In complex genetic circuits or in the simplest case overexpression of a certain gene, the effect of regulatory and expressed sequences arrayed on the same DNA molecule depends on their precise ordering, how they are linked across defined boundaries and their structural interaction. In addition, the ability to reliably stop transcription at a defined point is essential for a robust design. Avoiding context effects is currently the object of an intense engineering effort that has been reviewed recently.[14]

As reviewed above, read-through transcription by T7RNAP due to poor termination at the T7 phage-derived class I terminator TΦ is an issue of biotechnological relevance. In the course of this work, we have characterized the TE of 13 different terminator design principles *in vitro* with the aim to design a termination signal with improved properties compared to the T7TΦ wild-type. Different combinations of class I (T3 TΦ,[15] T7 TΦ,[8] synthetic T7 TΦ), class II (T7-CJ,[16] VSV[17,18]), and multiclass rrnBT1[19] termination signals were generated, and the construct with the highest TE was further characterized under industrial relevant conditions in fed-batch cultivations using human superoxide dismutase (SOD) as a model protein and the *recA*$^-$ *Escherichia coli* HMS174(DE3) as host.

RESULTS AND DISCUSSION

***In Vitro* Determination of Termination Efficiency.** In order to characterize different termination signal designs, the conventional T7TΦ termination signal was evaluated first using capillary electrophoresis (for an overview on this method see Figure 1). Here, wild-type (wt) T7TΦ is 130 bp downstream of the *sod* stop codon and TE was determined to be 79% for the pET30a⟨SOD⟩ reference plasmid (Figure 2/A). To test different terminators we generated a pET30a derivative, wherein the T7TΦ signal was deleted, denominated pET30a⟨SOD⟩ΔT7TΦ. In a first experiment we reintroduced

dx.doi.org/10.1021/sb5000115 | *ACS Synth. Biol.* 2015, 4, 265−273

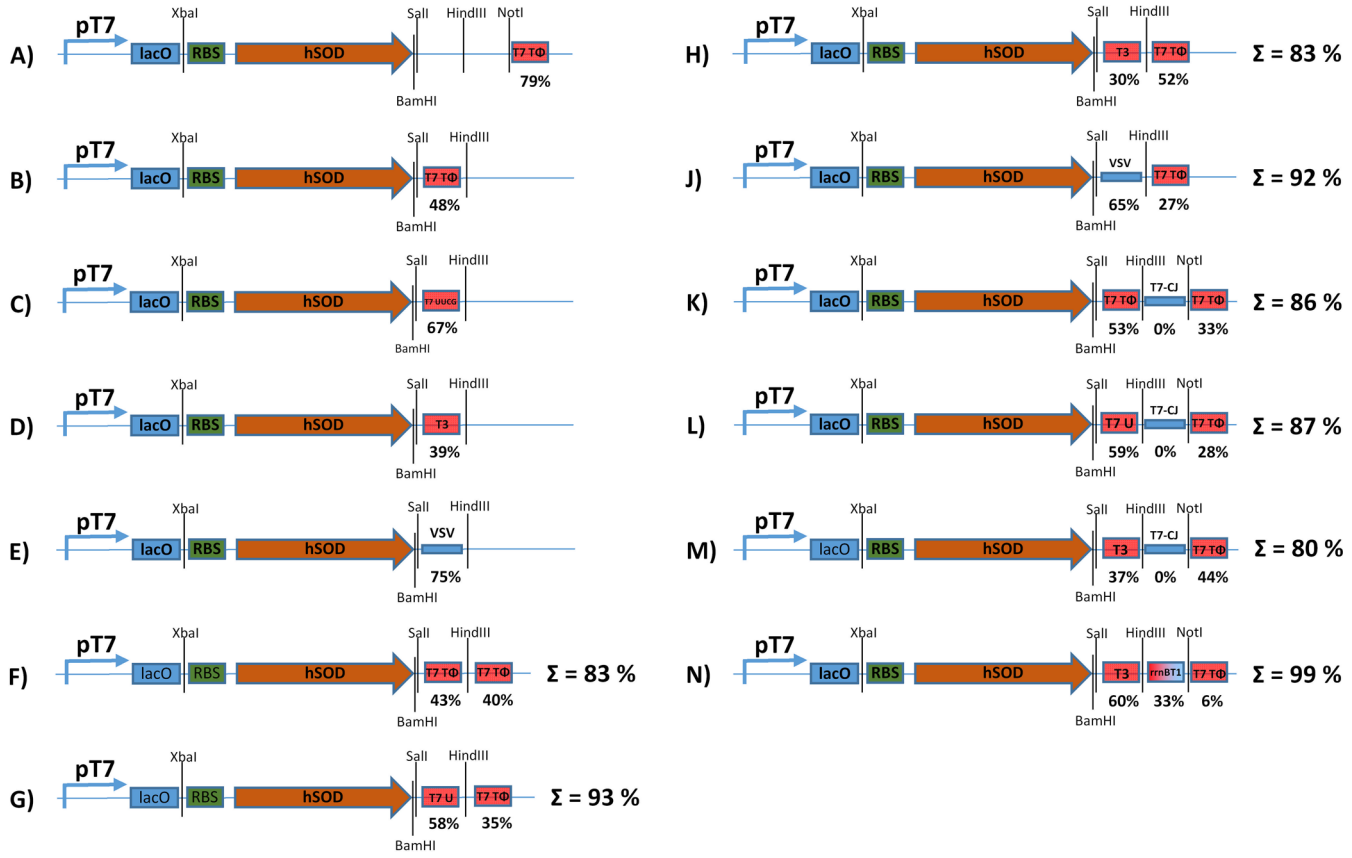

Figure 2. Different terminator design principles. Recognition sites for restriction enzymes are indicated by tick marks. Termination efficiency (TE) is indicated in bold letters for single terminators, for combination of different terminators the sum (Σ) of all single TE is indicated on the right. The improved T7UUCG is indicated by T7 U in this figure.

the T7TΦ at a different position (the fragment cloned was 67 bp in size including the stem-loop and U-tract and 7 bp up- and downstream of this sequence), 25 bp downstream of the *sod* stop codon, using restriction enzymes (RE) *Sal*I and *Hin*dIII (see Figure 2/B). When the signal was relocated the TE decreased to a value of 48%, thereby confirming the strong upstream and downstream sequence contextuality, as reported previously.[12] T7TΦ forms an extraordinary stable hairpin structure with an extended stem structure, resulting in a high ΔG value of −23 kcal/mol. RNA hairpin structures are the essential structural feature within intrinsic termination signals. The wt T7TΦ terminator contains a loop sequence of six nucleotides and an unpaired region comprising two unpaired G-U residues. We therefore engineered an artificial termination signal (UUCG-T7TΦ) that exhibits some modifications compared to the wt terminator, resulting in a higher overall ΔG value. The hexanucleotide loop was exchanged for the strong tetranucleotide loop sequence UUCG. In addition, the unpaired region within the stem structure was deleted by the presence of G-C base pairs instead of G-U (see Figure 3 for a detailed comparison). Hairpins containing the UUCG sequence in the loop are more stable compared to control hairpins and in addition UUCG serves as a strong nucleation site that reduces ΔG for loop closure, making that sequence widely distributed among hairpins.[20] When cloned 25 bp downstream of the *sod* stop codon using REs *Sal*I and *Hin*dIII, the TE of UUCG-T7TΦ was determined to be 67% (Figure 2C). The third class I terminator we tested was the T3TΦ (Figure 2D) having a TE of 39%. In addition to the class I single terminators, we also

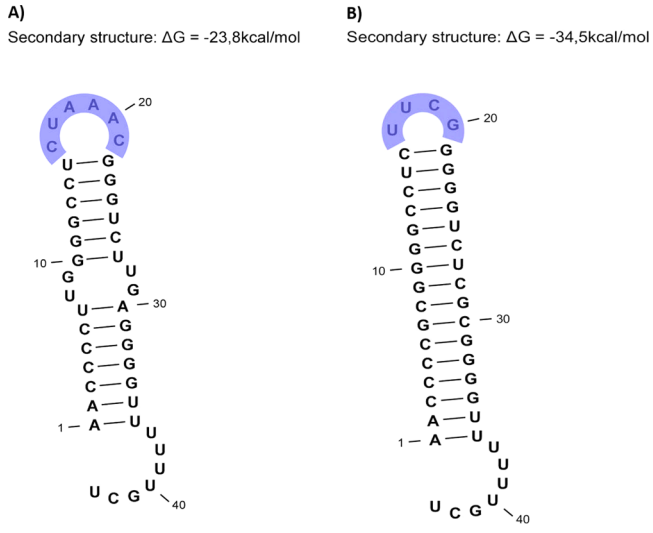

Figure 3. Comparison of the wt T7TΦ and the synthetic UUCG-T7TΦ folded as RNA.

tested a class II termination signal derived from the vesicular stomatitis virus (VSV). VSV was able to terminate T7RNAP with 75% efficiency (Figure 2E). We then started to test combinations of two different termination signals (Figure 2F–J) and identified the UUCG-T7TΦ/T7TΦ tandem terminator with a TE of 93% (Figure 2G) as the best performing terminaton signal. In a further attempt to increase the TE, the T7RNAP 8 bp pausing signal, found in the concatemer

dx.doi.org/10.1021/sb5000115 | *ACS Synth. Biol.* 2015, 4, 265–273

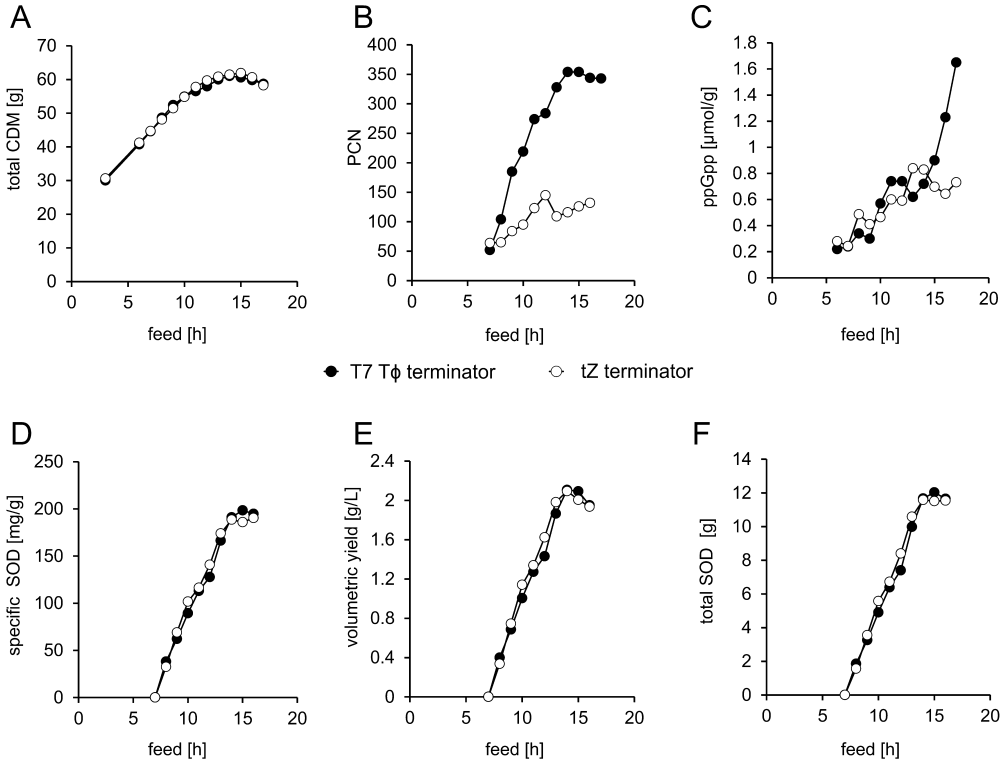

Figure 4. Process data full induction (20 μmol IPTG/g CDM): (A) Total cell dry mass (CDM) expressed in g/L. (B) Plasmid copy number (PCN) expressed in plasmids per genome. (C) Concentration of the alarmone ppGpp expressed in μmol/g CDM. (D) Specific content of SOD, determined by ELISA, expressed in mg/g CDM. (E) Volumetric yield of SOD expressed in g/L. (F) Total SOD expressed in g. Time after starting feed mode is shown on the *x*-axis. Filled circles correspond to data obtained with the conventional T7 TΦ, as found in pET30a; open circles correspond to data obtained with the triple terminator tZ.

junctions of replicating T7 DNA (T7-CJ), was tested in combination with the class I termination signals (T7TΦ, UUCG-T7TΦ, T3TΦ). T7-CJ was not able to further increase TE (Figure 2J–L). Surprisingly, the putative sequence even decreased overall termination in two cases (Figure 2L, M). Finally, a complex termination signal (tZ, Figure 2N) comprising the artificial UUCG-T7TΦ terminator, the T1 termination signal of the *rrnB* gene and the T7TΦ was constructed. The overall TE of tZ was determined to be 99%, thereby showing a 20% increase of TE when compared to the wt T7TΦ (Figure 2A vs N).

20-L Labscale Bioreactor Cultivations. pET30a⟨SOD⟩ has been recently used as a reference system.[13,21] Therefore, we decided to characterize the tZ termination signal, using the modified pET30a⟨SOD-tZ⟩, in fed batch fermentations. Whenever assaying plasmid-mediated effects, it is of critical importance to use *recA*$^-$ host strains to prevent segregational instabilities during fermentation.[22] For this reason HMS174-(DE3)[23] was used as a host. This strain provides the *recA1* mutation in an *E. coli* K-12 background and prevents plasmid multimerization and consequently plasmid loss.[24]

Two different induction schemes were evaluated: single-pulse full induction using 20 μmol IPTG/g cell dry mass (CDM) and limited induction, operating at a constant ratio of 0.9 μmol IPTG/g CDM using an exponential inducer feed.[25]

When full induction was performed (Figure 4), the differences between pET30a⟨SOD⟩ and pET30a⟨SOD-tZ⟩ in host cell response were only observable at the level of the plasmid copy number (PCN) (Figure 4B) and the ppGpp level (Figure 4C). The levels in CDM (Figure 4A) and the SOD protein related parameters (Figure 4D–F) remained unaffected. Interestingly, the PCN was reduced 3-fold for pET30a⟨SOD-tZ⟩ when compared at time point 14 h (corresponding to the maximal volumetric yield of 2.1 g/L). Full induction exerts a major metabolic burden on the host cell thereby leading to the total collapse of the host cell metabolism. It can be assumed that any positive effect (e.g. a lower PCN) is outweighed by the immense mRNA load processed by T7RNAP under those conditions.

When limited induction was performed, we observed a slight increase in CDM for pET30a⟨SOD-tZ⟩ (Figure 5A). This increase in cell growth was reflected by a much lower PCN (Figure 5B) and, consequently, a lower metabolic burden, indicated by a decrease in ppGpp concentrations (Figure 5C). In the case of the reference plasmid pET30a⟨SOD⟩, the PCN reached a maximum of 220 plasmids/genome 16 h after starting the feed mode, constituting a nearly 2-fold increase in PCN when compared to pET30a⟨SOD-tZ⟩, harboring the improved tZ termination signal. We anticipate that this much lower PCN is due to the improved TE of tZ that consequently decreases read-trough transcription into the adjacent plasmid origin of replication (ori). When we had acloser look on the SOD protein yields, we observed a 1.3-fold increase in specific SOD yield (Figure 5D), a 1.6-fold increase in volumetric yield (Figure 5E), and, consequently, a 1.6-fold increase in total SOD (Figure 5/F) for pET30a⟨SOD-tZ⟩ when compared to the pET30a⟨SOD⟩ reference 29 h after starting the feeding mode. This finding is in accordance with our previous publications where we found that lowering the overall metabolic burden (e.g., by lowering the PCN) is beneficial for the overall expression system performance.[13] We also performed a detailed investigation on the soluble and insoluble SOD protein content

dx.doi.org/10.1021/sb5000115 | *ACS Synth. Biol.* 2015, 4, 265–273

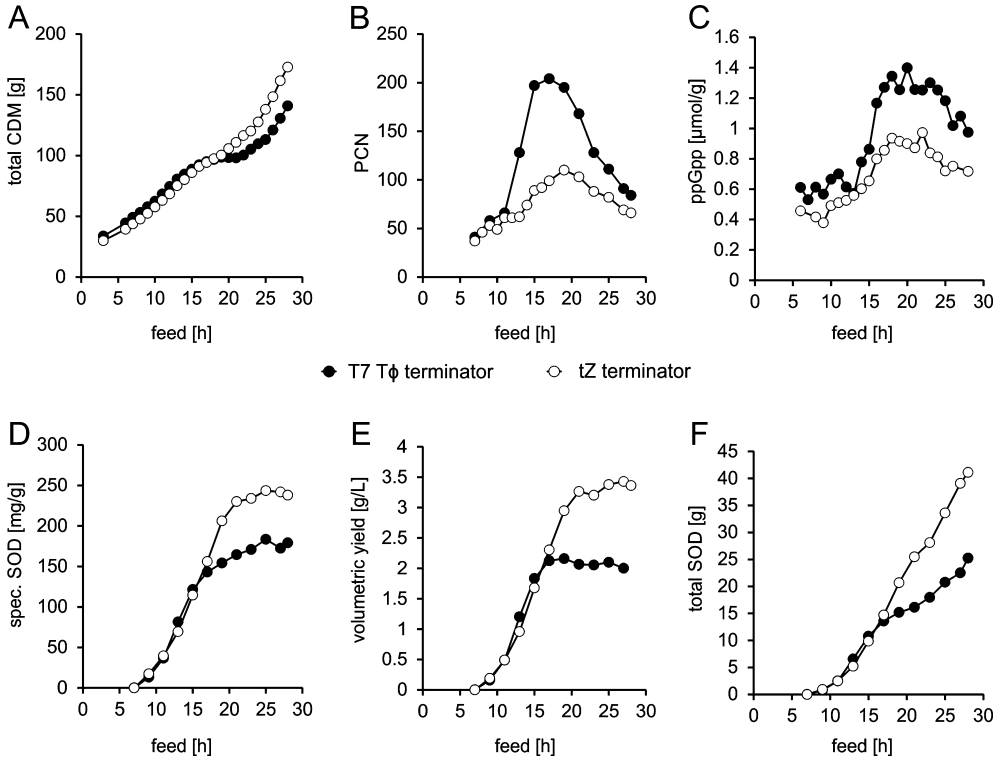

Figure 5. Process data limited induction (0.9 μmol IPTG/g CDM): (A) Total cell dry mass (CDM) expressed in g/L. (B) Plasmid copy number (PCN) expressed in plasmids per genome. (C) Concentration of the alarmone ppGpp expressed in μmol/g CDM. (D) Specific content of SOD, determined by ELISA, expressed in mg/g CDM. (E) Volumetric yield of SOD expressed in g/L. (F) Total SOD expressed in g. Time after starting feed mode is shown on the *x*-axis. Filled circles correspond to data obtained with the conventional T7 TΦ, as found in pET30a; open circles correspond to data obtained with the triple terminator tZ.

(Figure 6). The content of soluble and insoluble protein (inclusion bodies, IB) is heavily influenced by the induction

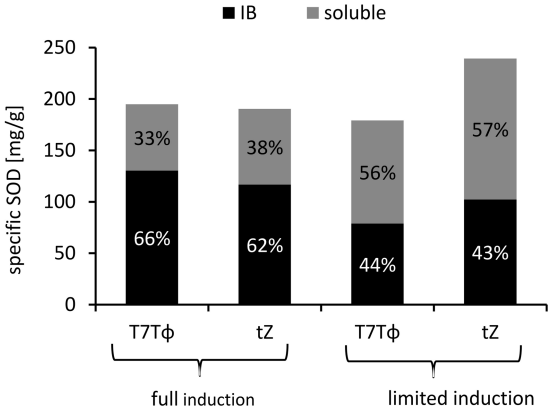

Figure 6. Comparison of soluble and insoluble SOD shown for the end of the process (16 h and 28 h) for full induction and limited induction regime and for the conventional T7 TΦ and the triple tZ terminator.

strength and strategy. In the experiments performed using full induction soluble SOD protein content at the end of the process (16 h in feed mode) was around 35%. The situation drastically changed when limited induction was used. Here, we observed approximately 60% of total protein in soluble form at the end of the process (29 h in feed mode). Concerning the tZ termination signal, we did not observe a significant influence on protein solubility. We have also tested the pET30a⟨SOD-tZ⟩ plasmid in BL21(DE3). Unlike HMS174(DE3), BL21(DE3) has a *recA*$^+$ genotype, characterized by rapid plasmid loss during limited and full induction, and therefore, positive effects due to improved TE are less pronounced in this strain although the increase in PCN is again significantly decreased (for details see Supporting Information S2).

In one of our former studies,[13] we revealed that a high gene dosage is detrimental to the host cell and that a single copy expression system, where the gene of interest is integrated into the host genome can perform better than a multicopy plasmid-based expression system. In the former referenced publication, we have shown that the metabolic burden is caused mostly by high mRNA levels of the gene of interest that prevent host intrinsic mRNAs from being translated. In the case of HMS174(DE3)pET30a⟨SOD-tZ⟩, when limited induction is performed (Figure 5/B), a significant difference in PCN 12 h after starting the feed mode is observable. At this time point, HMS174(DE3)pET30a⟨SOD⟩ shows a steep increase in PCN. This increase in PCN constitutes a severe load for the host cells since a higher PCN means higher mRNA levels of the gene of interest and lesser host intrinsic mRNAs are successfully translated into protein.[13] This increase in PCN is consequently transformed into a decrease in cell growth, observable with a delay, 16 h after starting the feeding mode (Figure 5A). With HMS174(DE3)pET30a⟨SOD⟩, we observed a plateau (Figure 5A, hours 16−21) in CDM whereas HMS174(DE3)-pET30a⟨SOD-tZ⟩ continues growing due to the lower PCN and consequently reduced metabolic burden. The time point where HMS174(DE3)pET30a⟨SOD⟩ ceases growth (16 h after starting feed mode) correlates with the divergence of the product titers (Figure 5D−F) between pET30a⟨SOD⟩ and

dx.doi.org/10.1021/sb5000115 | *ACS Synth. Biol.* 2015, 4, 265−273

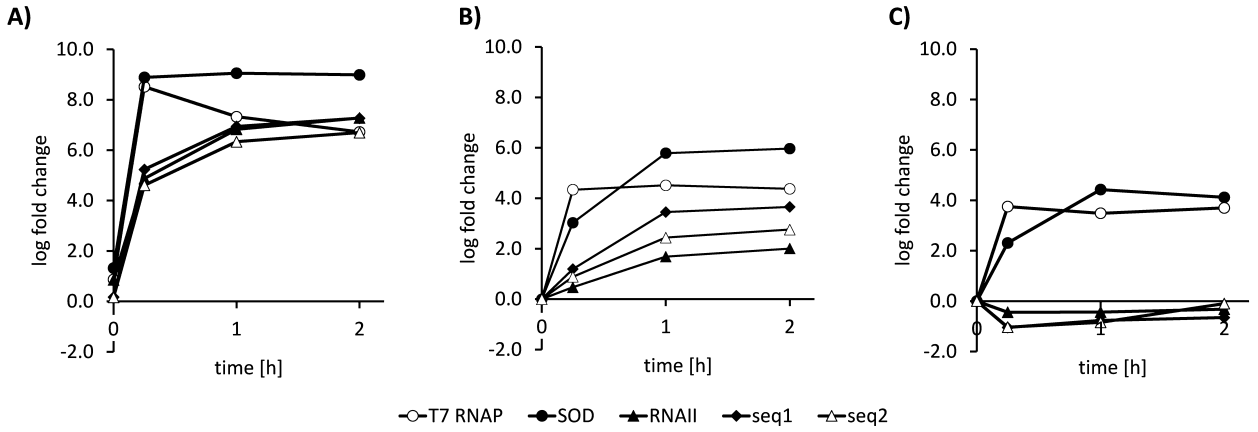

Figure 7. Log-fold change of different nCounter probes shown for different induction regimes and terminators. (A) Full induction with conventional T7 TΦ. (B) Limited induction with conventional T7 TΦ. (C) Limited induction with triple tZ terminator.

pET30a⟨SOD-tZ⟩. We therefore conclude that the tZ termination signal is capable of preventing the steep increase in PCN, as observable for pET30a⟨SOD⟩, and thereby reduces the metabolic burden exerted on the host cell.

Quantification of RNA Levels. To further characterize the phenomenon of read through transcription, we had a close look on transcription levels using the Nanostring nCounter technology.[26] We evaluated five different probes sets for transcription levels of T7RNAP, SOD, the primer for plasmid replication RNAII, and two plasmid backbone sequences seq1 and seq2. More information on the nucleotide sequences of the probe sets and the position of the probes on the plasmid backbone can be found in the Supporting Information S3 and in the Supporting Information S1/Figure S1.

When full induction was performed T7RNAP and SOD showed a log-fold change of >8 shortly after induction for pET30a⟨SOD⟩. All plasmid associated probes followed the same increase in log-fold change with a slightly lower fold-change of >6 (Figure 7A). When limited induction was performed, log-fold changes for T7RNAP and SOD were lower (Figure 7B and C). For the conventional pET30a⟨SOD⟩, plasmid-associated probes are still up-regulated, indicated by a log-fold change of >2 for RNAII, seq1 and seq2 (Figure 7B). When pET30a⟨SOD-tZ⟩ was used, no up-regulation of plasmid associated probes was observable indicating that read-through transcription indeed leads to significant changes in the abundance of the RNAII replication primer (Figure 7C).

Conclusion. By designing a termination signal with an improved TE compared to the wt T7 terminator, we have been able to significantly reduce read-through by T7RNAP and thereby improve fermentation characteristics and product yields. Failure to terminate transcription efficiently constitutes a major problem in plasmid-based genetic devices due to read-through into the plasmids origin of replication. In our specific case, we observed an increase in PCN, but the effect generated is very likely dependent on the directionality of the ori, causing either an increase or a decrease in PCN.

One explanation for an increase of PCN in the pET30a backbone setting could be the fact that the inhibitor of plasmid replication, RNAI (for a review on the control of DNA replication in ColE1-like plasmids see[27]), is encoded on the same strand as the GOI (see Figure 7A). Head-to-tail collision of T7RNAP with the *E. coli* RNAP could prevent functional transcription of RNAI due to the high processivity of T7RNAP. This would mean that plasmid DNA replication is initiated more often because lesser RNAI molecules are available to inhibit initiation of replication. Another possibility for interference would be head-to-head collisions of RNA and DNA polymerases,[28] consequently delaying DNA replication and thereby favoring plasmid loss.

Overall, the termination signal described herein has the potential to avoid read-through transcription by T7RNAP when used instead of the major late T7 terminator, TΦ. Consequently, expression of genes driven by T7RNAP becomes less invasive due to the reduction of interference with the PCN leading to increased robustness during bioreactor cultivations.

METHODS

Strains and Plasmids. *Escherichia coli* K-12 NEB5-α [*fhuA2Δ(argF-lacZ)U169 phoA gln V44 Φ80 Δ(lacZ)M15 gyrA96 recA1 relA1 endA1 thi-1 hsdR17*] was obtained from New England Biolabs (Ipswich, MA, U.S.A.) and used for all cloning procedures. *Escherichia coli* K-12 HMS174(DE3) [F^- recA1 hsdR(r_{K12}^- m_{K12}^+) (DE3) (Rif^R)] (Novagen, subdivision of Merck KgaA, Germany) was used as a plasmid host in fed-batch fermentations. Restriction enzymes and other modifying enzymes were purchased from New England Biolabs and used according to the manufacturer's recommendations. pET30a⟨-SOD⟩ or pET30a⟨SOD⟩Δ*T7*TΦ were derived by subcloning of the *Homo sapiens superoxide dismutase 1* gene [GenBank: BT006676.1] from pET11aSOD, described elsewhere,[29] using XbaI and *Bam*HI. All termination signals were either cloned using the restriction enzymes *Sal*I/*Hin*dIII or *Hin*dIII/NotI (see Figure 2). A detailed list of all primers used can be found in the Supporting Information S1.

***In Vitro* Transcription Assay.** *Sample Preparation.* *In vitro* determination of TE was performed using AmpliScribe T7 High Yield Transcription Kit from Epicenter Biotechnologies (Epicenter, subdivision of Illumina, CA, U.S.A.). For *in vitro* transcription assays plasmid DNA purified with QIAfilter Plasmid Midi kit (Qiagen, Hilden, Germany) was used as a template. Prior to transcription the templates were linearized by restriction digest with *Sma*I. The *Sma*I site is located about 1000 bp downstream of the MCS of pET30a, representing the longest possible transcription product. Distinct template DNA (2 μg) was digested with *Sma*I for 3 h at 25 °C. Subsequently the restriction enzyme was inactivated by incubation at 65 °C for 20 min and the reaction mixture was purified with Wizard SV Gel and PCR Clean-Up System. Linearized and purified

dx.doi.org/10.1021/sb5000115 | *ACS Synth. Biol.* 2015, 4, 265−273

plasmid DNA (200 ng) was used for subsequent *in vitro* transcription. The reaction contained the following components: 1× Ampliscribe T7 reaction buffer, 10 ng/μL template DNA, 7.5 mM ATP, 7.5 mM CTP, 7.5 mM GTP, 7.5 mM UTP, 10 mM DTTs, and 2 μL Ampliscribe T7 enzyme solution in a final volume of 20 μL. The whole transcription approach was incubated at 37 °C for 2−3 h. Subsequently the optional DNase I digest was carried out in order to get rid of template DNA. For that purpose 1 μL of DNase I solution (1 U/μL) was added to the *in vitro* transcription reaction mixture and digest was done for additional 15 min at 37 °C. Finally, RNA was purified and isolated using chloroform/phenol extraction and isopropanol precipitation.

Transcription Analysis and Calculation of Termination Efficiency. Purified RNA samples were analyzed according to their size and quantity using the Bioanalyzer 2100 (Agilent Technologies, CA, U.S.A.). For separation and quantification of *in vitro* transcribed RNA the Agilent RNA 6000 Nano LabChip kit was used. Sample preparation and analysis was done according to the manufacturer's recommendations. For all runs approximately 1 μL containing 200 ng of RNA were loaded on the chip. Each *in vitro* transcription assay was verified by loading at least 3 samples on one chip. RNA samples obtained from one transcription assay were also verified by loading on two different chips. In both cases standard deviation of calculated termination efficiency (TE) varied in a very small range and never exceeded ±0.4. In rare cases TE was also calculated from different *in vitro* transcription assays, whereby calculated TE showed higher standard deviation values of about ±1%. After separation of RNA transcripts according to their size the amount of the respective RNA fraction was assessed by calculation of the peak area and subsequent comparison to ladder area. For assessing the termination efficiency the amount of RNA has to be transferred into molar ratios. Termination efficiencies were calculated as the molar ratio between terminated transcript and the sum of terminated and read-through transcripts, and an average of at least three measurements was taken.

Quantitation of RNA Levels. *RNA Isolation from Fermentation Samples.* Samples were taken between feed hour 7 and 16 for the plasmid-based system and between feed hour 7 and 28 for the plasmid-free system. For RNA isolation samples were drawn directly into a 5% phenol−ethanol stabilizing solution and split into aliquots corresponding to about 3 mg CDM. Cell suspension was centrifuged for 2 min at ∼11 000*g* at 4 °C. The supernatant was discarded, and the pellet was immediately frozen at −80 °C. RNA was isolated by TRIzol reagent (Invitrogen, CA, U.S.A.) pulping and chloroform (Sigma-Aldrich, MI, U.S.A.) extraction according to the modified protocol described by Hedge and co-workers.[30] The quality of RNA was checked on a RNA1000 LabChip using the Agilent Bioanalyzer 2100 according to the protocol of the supplier (Agilent Bioanalyzer, Application Guide), and the RNA concentration was determined with the NanoDrop1000 (Thermo Fisher Scientific, MA, U.S.A.).

NanoString nCounter Analysis System. The Nanostring nCounter technology uses molecular barcodes and microscopic imaging to detect and count up to several hundred unique transcripts in one hybridization reaction. Each color-coded barcode is attached to a single target-specific probe corresponding to a gene of interest. Barcodes hybridize directly to their corresponding target molecules and can be individually counted without the need for amplification−providing very sensitive digital data.

RNA was isolated as described above and analyzed using the NanoString nCounter gene expression system, which captures and counts individual RNA transcripts. Advantages over existing platforms include direct measurement of RNA expression levels without enzymatic reactions or bias, sensitivity coupled with high multiplex capability, and digital readout. The sensitivity of the NanoString nCounter gene expression system is similar to that of real-time PCR. nCounter data can be found in Supporting Information S3.

Medium, Composition, Cultivation, and Sampling. A minimal media described by Marisch et al.[21] calculated to produce 22.5 g CDM in the batch phase and another 237 g CDM during feed phase was used for cultivation in a 20 L (14 L net volume, 4 L batch volume) computer controlled bioreactor (MBR; Wetzikon, Switzerland) equipped with standard control units (Siemens PS7, Intellution iFIX). The pH was maintained at a set-point of 7.0 ± 0.05 by addition of 25% ammonia solution (MERCK), the temperature was set to 37 °C ± 0.5 °C. In order to avoid oxygen limitation the dissolved oxygen level was stabilized above 30% saturation by stirrer speed and aeration rate control. Foaming was suppressed by addition of 0.5 mL antifoam (PPG 2000) per liter media. For inoculation, a deep frozen (−80 °C) working cell bank vial, was thawed and 1 mL (optical density OD_{600} = 1) was transferred aseptically with 30 mL 0.9% NaCl solution to the bioreactor. The fed-batch regime with an exponential substrate feed was used to provide a constant growth rate of 0.1 h^{-1} over 4 doubling times. One doubling time past feed start the culture was induced with isopropyl-β-D-thiogalactopyranosid (IPTG) (GERBU Biotechnik, Germany) following two different induction strategies. The single pulse induction of 20 μmol IPTG per gram calculated final CDM aimed at a full induction and high expression levels. The limited induction with continuous supply of physiology tolerable amounts of inducer in a constant ratio to CDM (0.9 μmol/g) aimed at control of the expression level.[25]

Sampling for Process Parameter Analysis. Optical density at 600 nm was measured with a spectrophotometer (Amersham Biosciences Ultrospec 500 Pro). CDM was determined by centrifugation of 2 × 10 mL of cell suspension. The supernatant was transferred to an Eppendorf vial, frozen at −20 °C, and analyzed separately by HPLC. The cells were washed with 7 mL distilled water and after resuspension transferred to two preweighed beakers. The beakers were dried at 105 °C for 24 h and reweighed. Plasmid copy number (PCN) was calculated from plasmid and chromosomal DNA.[31] Plasmid DNA was isolated from the bacterial cells using a commercial miniprep kit (Promega SV Wizard) and quantified with the Agilent Bioanalyser DNA 7500 LabChip Kit. To estimate the rate of plasmid loss during purification, samples were spiked with pUC19 DNA. Total DNA was determined by fluorescence assay using HOECHST dye H33258 after cell disintegration with lysozyme and sodium dodecyl sulfate.[32] Sample preparation for the determination of nucleotides was performed as described by Cserjan and co-workers and for quantification reversed-phase HPLC was used.[33] The recombinant protein was quantified via SOD-ELISA,[34] and the ratio between soluble protein and inclusion bodies was determined by SDS-PAGE, as previously described.[35]

dx.doi.org/10.1021/sb5000115 | *ACS Synth. Biol.* 2015, 4, 265−273

■ ASSOCIATED CONTENT

Supporting Information

This material is available free of charge *via* the Internet at http://pubs.acs.org.

■ AUTHOR INFORMATION

Corresponding Author

*Email: gerald.striedner@boku.ac.at.

Author Contributions

[§]J.M. and A.W. contributed equally. J.M. and A.W. participated in the design of the study and were involved in analysis and interpretation. J.M. and G.S. wrote the manuscript. M.C.P. was involved in the off-line process analytics (ELISA, SDS-PAGE, PCN). All authors read and approved the final manuscript.

Notes

The authors declare no competing financial interest.

■ ACKNOWLEDGMENTS

This work was supported by the Federal Ministry of Traffic, Innovation and Technology (bmvit), the Federal Ministry of Economy, Family and Youth (BMWFJ), the Styrian Business Promotion Agency SFG and the Standortagentur Tirol and ZIT—Technology Agency of the City of Vienna through the COMET-Funding Program managed by the Austrian Research Promotion Agency FFG. The technical assistance of Florian Strobl and Norbert Auer is highly appreciated.

■ REFERENCES

(1) Davanloo, P., Rosenberg, A. H., Dunn, J. J., and Studier, F. W. (1984) Cloning and expression of the gene for bacteriophage T7 RNA polymerase. *Proc. Natl. Acad. Sci. U.S.A. 81*, 2035−2039.

(2) An, W., and Chin, J. W. (2009) Synthesis of orthogonal transcription−translation networks. *Proc. Natl. Acad. Sci. U.S.A. 106*, 8477−8482.

(3) Shis, D. L., and Bennett, M. R. (2013) Library of synthetic transcriptional AND gates built with split T7 RNA polymerase mutants. *Proc. Natl. Acad. Sci. U.S.A. 110*, 5028−5033.

(4) Temme, K., Hill, R., Segall-Shapiro, T. H., Moser, F., and Voigt, C. A. (2012) Modular control of multiple pathways using engineered orthogonal T7 polymerases. *Nucleic Acids Res. 40*, 8773−8781.

(5) McAllister, W. T., Morris, C., Rosenberg, A. H., and Studier, F. W. (1981) Utilization of bacteriophage T7 late promoters in recombinant plasmids during infection. *J. Mol. Biol. 153*, 527−544.

(6) d'Aubenton Carafa, Y., Brody, E., and Thermes, C. (1990) Prediction of rho-independent *Escherichia coli* transcription terminators. A statistical analysis of their RNA stem-loop structures. *J. Mol. Biol. 216*, 835−858.

(7) Carter, A. D., Morris, C. E., and McAllister, W. T. (1981) Revised transcription map of the late region of bacteriophage T7 DNA. *J. Virol. 37*, 636−642.

(8) Dunn, J. J., and Studier, F. W. (1983) Complete nucleotide sequence of bacteriophage T7 DNA and the locations of T7 genetic elements. *J. Mol. Biol. 166*, 477−535.

(9) Du, L., Gao, R., and Forster, A. C. (2009) Engineering multigene expression *in vitro* and *in vivo* with small terminators for T7 RNA polymerase. *Biotechnol. Bioeng. 104*, 1189−1196.

(10) Du, L., Villarreal, S., and Forster, A. C. (2012) Multigene expression *in vivo*: Supremacy of large versus small terminators for T7 RNA polymerase. *Biotechnol. Bioeng. 109*, 1043−1050.

(11) Chen, Y. J., Liu, P., Nielsen, A. A., Brophy, J. A., Clancy, K., Peterson, T., and Voigt, C. A. (2013) Characterization of 582 natural and synthetic terminators and quantification of their design constraints. *Nat. Methods 10*, 659−664.

(12) Cambray, G., Guimaraes, J. C., Mutalik, V. K., Lam, C., Mai, Q. A., Thimmaiah, T., Carothers, J. M., Arkin, A. P., and Endy, D. (2013) Measurement and modeling of intrinsic transcription terminators. *Nucleic Acids Res. 41*, 5139−5148.

(13) Mairhofer, J., Scharl, T., Marisch, K., Cserjan-Puschmann, M., and Striedner, G. (2013) Comparative transcription profiling and in-depth characterization of plasmid-based and plasmid-free *Escherichia coli* expression systems under production conditions. *Appl. Environ. Microbiol. 79*, 3802−3812.

(14) Cardinale, S., and Arkin, A. P. (2012) Contextualizing context for synthetic biology—Identifying causes of failure of synthetic biological systems. *Biotechnol. J. 7*, 856−866.

(15) Sengupta, D., Chakravarti, D., and Maitra, U. (1989) Relative efficiency of utilization of promoter and termination sites by bacteriophage T3 RNA polymerase. *J. Biol. Chem. 264*, 14246−14255.

(16) Harvey, B., Korus, M., and Goldman, E. (1999) The T7 concatemer junction sequence interferes with expression from a downstream T7 promoter *in vivo*. *Gene Expr. 8*, 141−149.

(17) Whelan, S. P., Ball, L. A., Barr, J. N., and Wertz, G. T. (1995) Efficient recovery of infectious vesicular stomatitis virus entirely from cDNA clones. *Proc. Natl. Acad. Sci. U.S.A. 92*, 8388−8392.

(18) Lyakhov, D. L., He, B., Zhang, X., Studier, F. W., Dunn, J. J., and McAllister, W. T. (1998) Pausing and termination by bacteriophage T7 RNA polymerase. *J. Mol. Biol. 280*, 201−213.

(19) Orosz, A., Boros, I., and Venetianer, P. (1991) Analysis of the complex transcription termination region of the *Escherichia coli* rrnB gene. *Eur. J. Biochem. 201*, 653−659.

(20) Tuerk, C., Gauss, P., Thermes, C., Groebe, D. R., Gayle, M., Guild, N., Stormo, G., d'Aubenton-Carafa, Y., Uhlenbeck, O. C., Tinoco, I., Jr., et al. (1988) CUUCGG hairpins: Extraordinarily stable RNA secondary structures associated with various biochemical processes. *Proc. Natl. Acad. Sci. U.S.A. 85*, 1364−1368.

(21) Marisch, K., Bayer, K., Cserjan-Puschmann, M., Luchner, M., and Striedner, G. (2013) Evaluation of three industrial *Escherichia coli* strains in fed-batch cultivations during high-level SOD protein production. *Microb Cell Fact 12*, 58.

(22) Zhao, J. B., Wei, D. Z., and Tong, W. Y. (2007) Identification of *Escherichia coli* host cell for high plasmid stability and improved production of antihuman ovarian carcinoma × antihuman CD3 single-chain bispecific antibody. *Appl. Microbiol. Biotechnol. 76*, 795−800.

(23) Campbell, J. L., Tamanoi, F., Richardson, C. C., and Studier, F. W. (1979) Cloning of the T7 genome in *Escherichia coli*: Use of recombination between cloned sequences and bacteriophage T7 to identify genes involved in recombination and a clone containing the origin of T7 DNA replication. *Cold Spring Harb Symp. Quant Biol. 43* (Pt 1), 441−448.

(24) Field, C. M., and Summers, D. K. (2011) Multicopy plasmid stability: Revisiting the dimer catastrophe. *J. Theor. Biol. 291*, 119−127.

(25) Striedner, G., Cserjan-Puschmann, M., Pötschacher, F., and Bayer, K. (2003) Tuning the transcription rate of recombinant protein in strong *Escherichia coli* expression systems through repressor titration. *Biotechnol. Prog. 19*, 1427−1432.

(26) Geiss, G. K., Bumgarner, R. E., Birditt, B., Dahl, T., Dowidar, N., Dunaway, D. L., Fell, H. P., Ferree, S., George, R. D., Grogan, T., James, J. J., Maysuria, M., Mitton, J. D., Oliveri, P., Osborn, J. L., Peng, T., Ratcliffe, A. L., Webster, P. J., Davidson, E. H., Hood, L., and Dimitrov, K. (2008) Direct multiplexed measurement of gene expression with color-coded probe pairs. *Nat. Biotechnol. 26*, 317−325.

(27) Davison, J. (1984) Mechanism of control of DNA replication and incompatibility in ColE1-type plasmids—A review. *Gene 28*, 1−15.

(28) Mirkin, E. V., and Mirkin, S. M. (2005) Mechanisms of transcription−replication collisions in bacteria. *Mol. Cell. Biol. 25*, 888−895.

(29) Kramer, W., Elmecker, G., Weik, R., Mattanovich, D., and Bayer, K. (1996) Kinetics studies for the optimization of recombinant protein formation. *Ann. N.Y. Acad. Sci. 782*, 323−333.

(30) Hegde, P., Qi, R., Abernathy, K., Gay, C., Dharap, S., Gaspard, R., Hughes, J. E., Snesrud, E., Lee, N., and Quackenbush, J. (2000) A concise guide to cDNA microarray analysis. *Biotechniques 29*, 548−554 556 passim..

(31) Breuer, S., Marzban, G., Cserjan-Puschman, M., Dürrschmid, E., and Bayer, K. (1998) Off-line quantitative monitoring of plasmid copy number in bacterial fermentation by capillary electrophoresis. *Electrophoresis 19*, 2474−2478.
(32) Rymaszewski, Z., Abplanalp, W. A., Cohen, R. M., and Chomczynski, P. (1990) Estimation of cellular DNA content in cell lysates suitable for RNA isolation. *Anal. Biochem. 188*, 91−96.
(33) Cserjan-Puschmann, M., Kramer, W., Duerrschmid, E., Striedner, G., and Bayer, K. (1999) Metabolic approaches for the optimization of recombinant fermentation processes. *Appl. Microbiol. Biotechnol. 53*, 43−50.
(34) Porstmann, T., Wietschke, R., Schmechta, H., Grunow, R., Porstmann, B., Bleiber, R., Pergande, M., Stachat, S., and Von Baehr, R. (1988) A rapid and sensitive enzyme immunoassay for Cu/Zn superoxide dismutase with polyclonal and monoclonal antibodies. *Clin. Chim. Acta 171*, 1−10.
(35) Laemmli, U. K. (1970) Cleavage of structural proteins during the assembly of the head of bacteriophage T4. *Nature 227*, 680−685.